Magnetic resonance imaging of cancer metabolism with hyperpolarized ^{13}C-labeled cell metabolites

R. L. Hesketh[1] and K. M. Brindle[1,2]
1. Cancer Research UK Cambridge Institute, Li Ka Shing Centre, Robinson Way, Cambridge, CB2 0RE.
2. Department of Biochemistry, University of Cambridge, Tennis Court Road, Cambridge, CB2 1GA.

Abstract

Hyperpolarization of ^{13}C-labeled substrates can increase their ^{13}C NMR signal by more than 10,000-fold, which has allowed magnetic resonance imaging (MRI) of metabolic reactions *in vivo*. This has already provided a unique insight into the dysregulated metabolic pathways and microenvironment of tumors. Perhaps the best known of the cancer-associated metabolic abberations is the Warburg effect, which has been imaged in patients using hyperpolarized [1-^{13}C]pyruvate. In clinical oncology there is a requirement to diagnose tumors earlier, better determine their aggressiveness and prognosis, identify novel treatment targets and detect response to treatment earlier. Here we consider some of the hyperpolarized substrates that have been developed and have the potential to meet these requirements and become the precision imaging tools of the future.

Introduction

For most cancers imaging is important for diagnosis, prognosis, guiding treatment and monitoring subsequent response. Computed tomography (CT) and magnetic resonance imaging (MRI) give anatomical information, but provide limited information about tumor biology. As personalized oncology becomes a reality, the development of functional imaging techniques is required to complement the range of emerging genetic and molecular tests.

Warburg's observation that tumor cells preferentially metabolize glucose to lactate in normoxia, rather than oxidize it in the TCA cycle, led him to falsely conclude that cancer was a metabolic disease caused by mitochondrial dysfunction [1]. Remarkably it took another 46 years for the first proto-oncogene, *SRC*, to be discovered, leading to the realization that cancer is a disease resulting from genetic mutation and instability [2]. We now know that some key metabolic pathways are under direct control of the most frequently mutated oncogenes and tumor suppressor

genes and, although the Warburg effect is a characteristic of many tumors, it is just one feature of the metabolic reprogramming that occurs and is required to support tumor growth [3,4].

Functional imaging techniques have been developed that non-invasively probe tissue biochemistry, many of which interrogate the dysregulated metabolic processes that are a hallmark of cancer [5]. A wide range of radiopharmaceuticals have been developed and employed clinically for use with positron emission tomography (PET) [6,7]. Whilst PET offers unrivalled sensitivity (in the femtomolar to picomolar range), the limitation is that the tracer and downstream metabolic products cannot be differentiated. Paradoxically, ^{1}H or ^{13}C magnetic resonance spectroscopy (MRS) are able to differentiate between metabolites but are limited by sensitivity [8].

Dissolution dynamic nuclear polarization (DNP) of ^{13}C labeled substrates can increase the signal-to-noise ratio in ^{13}C magnetic resonance spectra and spectroscopic images by $>10^4$, permitting real-time spectroscopy or spectroscopic imaging of the injected substrate and its conversion to downstream metabolic products (**Box 1**). Due to its position in the glycolytic pathway, favorable polarization levels and polarization lifetime, hyperpolarized [1-^{13}C]pyruvate has been the most widely used substrate in pre-clinical studies and has also been used in clinical studies [9,10]. It is transported into cells by monocarboxylate transporters (MCTs) and in tumors is reduced predominantly to lactate, in the reaction catayzed by lactate dehydrogenase (LDH). [1-^{13}C]alanine and ^{13}C-bicarbonate are also detectable in smaller quantities following pyruvate transamination and decarboxylation, respectively [11-13]. Various hyperpolarized substrates have been used to study cancer metabolism (Table 1 and Fig. 1). There are several recent comprehensive reviews of hyperpolarized MRI [14-17]. We focus here on recent applications of hyperpolarized MRI in oncology, which in some cases have the potential for clinical translation.

Box 1

Dissolution Dynamic Nuclear Polarization (DNP)

Hyperpolarization can be achieved in a number of ways but DNP has been the most widely used. Although it can in principle be used with any NMR-active nucleus the majority of studies have been performed with ^{13}C-labeled molecules because of the relatively long polarization lifetime for this nucleus and the possibility

of measuring metabolic fluxes with ^{13}C-labeled cell metabolites. The ^{13}C labeled substrate to be hyperpolarized is mixed with a stable radical and rapidly frozen to form a glass. At temperatures approaching 1 K, and in the presence of a strong magnetic field (> 3 Tesla), the electron spins on the radical are almost completely polarized. Excitation of the electron spin resonance by microwave irradiation results in transfer of the electron spin polarization to the nuclear spins. The hyperpolarized ^{13}C-labeled metabolite is then brought rapidly to room temperature, with substantial retention of the nuclear spin polarization in a process that involves injection of a super-heated aqueous solvent (~450 K) [16,18]. After dissolution the polarization lasts from seconds to a few minutes, depending on the molecule and the position of the ^{13}C nucleus within the molecule, with its half-life determined by the longitudinal relaxation time constant (T_1).

Screening, diagnosis and disease progression

Hyperpolarized imaging has already shown clinical diagnostic potential in a first-in-man study in prostate cancer [9]. An elevated [1-^{13}C]lactate/[1-^{13}C]pyruvate ratio was observed in tumor regions and in one patient a biopsy-proven tumor was identified by hyperpolarized imaging but not by multi-parametric ^{1}H-MRI [9].

In prostate cancer there is a requirement for new approaches to determine tumor aggressiveness. In men over sixty 30-70% are estimated to have prostate cancer but the vast majority require no treatment [19]. However, 30% of patients defined as being low-risk actually harbor higher-grade tumors that would benefit from early treatment [20]. As nearly 80% of cases present with localized disease [21], imaging with hyperpolarized [1-^{13}C]pyruvate is a potentially useful tool for determining the aggressiveness of these tumors. In a recent study [1-^{13}C]pyruvate was co-polarized with ^{13}C-urea (an agent for imaging perfusion) and injected into a transgenic mouse model of prostate adenocarcinoma (TRAMP). Both agents differentiated high- and low-grade tumors, with high-grade tumors showing increased lactate labeling and reduced perfusion but higher vascular permeability and ^{13}C urea washout [22].

At the other end of the cancer spectrum, pancreatic cancer has >90% mortality within 5 years of diagnosis, with early detection and surgery currently offering the only chance of survival [21]. In genetically engineered mouse models

[23,24] of pancreatic ductal adenocarcinoma the [1-^{13}C]alanine/[1-^{13}C]lactate ratio, following injection of hyperpolarized [1-^{13}C]pyruvate, was shown to decrease with disease progression [13]. Similarly, hepatocellular carcinoma has a mortality rate in excess of 95%, making it the second most common cause of cancer-mortality worldwide. However, localized tumors suitable for resection or ablation have a good prognosis [25]. Differentiation of small malignant tumors from benign tumors and cirrhotic liver is challenging but may be aided by metabolic imaging. In hepatoma cells glutamine uptake is 10-30 fold greater than in normal hepatocytes [26-28]. Following injection of hyperpolarized [5-^{13}C]glutamine, [5-^{13}C]glutamate could be detected *in vivo* in rat hepatomas but not in normal liver [29,30]. However, [5-^{13}C]glutamine does not polarize well and has a short T_1, and although there are techniques that can improve these characteristics slightly [31], they may ultimately limit clinical translation.

While it is unrealistic to suggest population-based screening with any cross-sectional imaging technique, let alone hyperpolarized MRI, it may be feasible for highly stratified groups, such as patients with hereditary cancer syndromes. The development of more sensitive and specific circulating biomarkers could also facilitate patient stratification prior to confirmation with imaging.

Tumor phenotyping

Isocitrate dehydrogenase (IDH)

Wild-type IDH catalyzes oxidative decarboxylation of isocitrate to α-ketoglutarate (α-KG). The most common mutation of IDH in cancer leads to a neomorphic function and the reduction of α-KG to D-2-hydroxyglutarate (2-HG), a metabolite present in very low concentrations in normal tissue and which has been termed an oncometabolite because of its effects on epigenetic modifications and gene expression [4]. IDH1 (the cytosolic isoform) is mutated in >70% of low-grade gliomas and non-invasive determination of IDH1 mutational status would change the approach to surgical resection [32]. Hyperpolarized [2-^{13}C]pyruvate allows visualization of TCA cycle metabolites and in IDH1 mutated cells there was reduced [5-^{13}C]glutamate labeling because of down-regulation of pyruvate dehydrogenase activity [33,34]. [1-^{13}C]2-HG has been observed in tumor models *in vivo* following injection of hyperpolarized [1-^{13}C]α-KG [35] and [1-^{13}C]glutamine [36].

ɣ-glutamyl-transpeptidase (GGT)

GGT is bound to the outer aspect of the plasma membrane, where it catalyzes degradation of extracellular glutathione to its constituent amino acids (glutamate, cysteine and glycine), which can then be used for intracellular glutathione synthesis. GGT is over-expressed in a variety of tumors where it may have a role in progression, invasion and drug resistance [37]. Cleavage of hyperpolarized ɣ-glutamyl-[1-^{13}C]glycine to [1-^{13}C]glycine, catalyzed by GGT, was measured in normal rat organs [38]. The next step will be to determine whether tumor over-expression of GGT can be detected.

Early Detection of Treatment Response

Early detection of treatment response could reduce the duration of ineffective therapies, decreasing costs and unnecessary side effects and facilitating an earlier switch to alternative treatments. Interim ^{18}FDG-PET-CT scans after one or two cycles of chemotherapy is now standard of care for most lymphomas [39-41]. There is also emerging evidence that early response can be detected with ^{18}FDG-PET in melanoma patients treated with the BRAF inhibitor vemurafenib or immune checkpoint inhibitors targeting CTLA-4 or PD1 [42-45]. However, overall there has been a reluctance to utilize ^{18}FDG-PET for this purpose, with some studies reporting lack of efficacy and because of exaggerated fears over repeated ionizing radiation exposure [46] and the poorly understood metabolic “flare effect” [47-49].

Hyperpolarized substrates avoid the use of ionizing radiation and, by using probes more specific than ^{18}FDG for cancer metabolism or the chemotherapeutic being used, may be more sensitive to early therapy induced changes in metabolism. So far [1-^{13}C]pyruvate has been the most thoroughly investigated hyperpolarized substrate for treatment response monitoring. Chemotherapy and radiotherapy have been observed to alter hyperpolarized [1-^{13}C]pyruvate metabolism in numerous animal models, usually leading to a decrease in lactate labelling[11,50-56]. Detection of treatment response in a prostate cancer patient was reported recently. Following six weeks of androgen deprivation therapy [1-^{13}C]lactate was virtually

undetectable. With ^{1}H-MRI, there were only small changes in the apparent diffusion coefficient of tissue water and tumor size [10].

However, a number of studies have failed to detect treatment response with [1-^{13}C]pyruvate or shown that it is less sensitive than tumor size measurements [57-59]. In these instances a different approach to response detection is required. Following injection of hyperpolarized [1,4 $^{13}C_2$]fumarate the detection of malate is a sensitive indicator of cell death [59,60]. Hydration of hyperpolarized [1,4 $^{13}C_2$]fumarate to malate, catalysed by fumarase, is seen in areas of necrosis, where increases in cell membrane permeability improve cell uptake of fumarate and result in leakage of fumarase into the extracellular space [60].

Tumor Microenvironment

pH

The acidic extracellular environment of tumors, which is often associated with tumor hypoxia, contributes to the malignant phenotype by upregulating signaling pathways promoting tumor growth, inflammation, angiogenesis and metastasis, whilst inhibiting immune cell activation, chemotherapeutic delivery to the tumor and radio-sensitivity [61].

Injection of hyperpolarized ^{13}C-bicarbonate results in the production of $^{13}CO_2$ and the extracellular pH and carbonic anhydrase activity can be determined from the $H^{13}CO_3^-/^{13}CO_2$ signal ratio [62,63]. Several hyperpolarized probes that exhibit pH-dependent chemical shifts have also been described. $^{15}N_2$-imidazole and several ^{15}N-pyridine derivatives have been hyperpolarized and tested *in vitro* with chemical shifts of up to 60 ppm per pH unit [64,65]. More recently [1,5-^{13}C]zymonic acid has been used *in vivo* to image the pH of multiple tissues [66].

Redox Status

Tumors generally have elevated production of reactive oxygen species (ROS), which promote tumor development and resistance to therapy [67]. To regulate increased ROS production, antioxidant production is also increased and several hyperpolarized probes have been used to probe these regulatory mechanisms. [1-^{13}C]alanine has been used to measure lactate/pyruvate ratio as a surrogate for the NAD^+/NADH ratio [68]. The pentose phosphate pathway (PPP) produces NADPH,

required by glutathione reductase to maintain levels of reduced glutathione, a key anti-oxidant. Flux through the PPP has been estimated in tumors by measuring [U-^{2}H, U-^{13}C]glucose conversion to 6-phosphogluconate, a PPP intermediate [69,70] and recently the production of $H^{13}CO_3^-$ was detected in mouse liver following injection of δ-[1-^{13}C]gluconolactone [71]. Ascorbic acid (AA) combats oxidative stress by reducing ROS and in the process producing dehydroascorbic acid (DHA). DHA can then be reduced back to AA *via* glutathione or NADPH dependent reactions. Hyperpolarized [1-^{13}C]dehydroascorbic acid and measurement of its reduction to [1-^{13}C]ascorbic acid has been used to probe intracellular redox status in a number of animal models of cancer [72-74].

Technical Developments

The transient nature of hyperpolarization limits it use to metabolic events occurring on a timescale of seconds to minutes. Furthermore, each excitation required to produce a spectrum or image results in further depletion of the hyperpolarization. 3D imaging sequences have been described recently that have improved the nominal spatial resolutions in lactate and pyruvate images to ≤0.003 cm^3, with image acquisition times of <2 s [75,76]. Improved polarizers and injection protocols could improve the signal available initially [16,77] and rapid removal of the radical, which dramatically prolongs polarization lifetime, has been achieved using a number of different methods [78,79]. Provided the sample remains at low temperature and in a relatively high magnetic field T_1s > 20 h are possible [78]. This would permit centralized substrate hyperpolarization followed by transport to multiple locations for clinical use, in a similar fashion to ^{18}F-labeled PET tracers, dispensing with the requirement to have a hyperpolarizer in close proximity to the MRI scanner.

Transferring polarization from hyperpolarized ^{13}C nuclei to spin-coupled ^{1}H nuclei can be used to further enhance signal detection. Dynamic ^{1}H imaging of lactate methyl protons following injection of [1-^{13}C]pyruvate was recently demonstrated *in vivo* [80]. The resulting signal enhancements are likely to be greater at the lower magnetic field strengths used in the clinic.

PET-MRI

PET-MRI combines improved soft tissue contrast with the functional information provided by both PET and MRI and is likely to be of particular use where MRI is already the anatomical imaging technique of choice e.g. in brain, liver and prostate [81]. Simultaneous hyperpolarized ^{13}C MRI and PET studies permit more extensive metabolic phenotyping of tumors, as already demonstrated in pre-clinical studies (Figure 2) [82-85]. ^{18}FDG can be used to measure the first two steps of glycolysis, cell uptake *via* the glucose transporters and irreversible trapping after phosphorylation by hexokinase. Therefore the combination of ^{18}FDG and [1-^{13}C]pyruvate may yield a single metric that estimates glucose uptake and its subsequent metabolism. For example, high ^{18}FDG uptake and low [1-^{13}C]lactate production may suggest that mitochondrial oxidation of glucose predominates, whereas high ^{18}FDG uptake and high [1-^{13}C]lactate labeling would be indicative of the Warburg effect. Studies so far have either demonstrated concordance between ^{18}FDG uptake and [1-^{13}C]lactate production [83,85] or that hyperpolarized tracers can have improved tumor specificity when compared to ^{18}FDG [82,84].

Conclusions

For a field still very much in its infancy a remarkable number of substrates have been hyperpolarized and have provided novel, pre-clinical insights into tumor metabolism *in vivo*. Hyperpolarized [1-^{13}C]pyruvate has already entered clinical trials and other substrates will undoubtedly follow. The major weakness is the transient nature of the signal, limiting studies to fast metabolic reactions in pre-defined body regions. Therefore it is very unlikely that hyperpolarized substrates will replace nuclear medicine techniques for staging metastatic cancers. However, its great strength is the potential for kinetic measurements of multiple enzymatic processes providing functional data. For use as a clinical biomarker, these data must be sufficiently sensitive and specific to inform treatment decisions, prognosis, or monitor treatment response in ways that are not possible by using circulating biomarkers or other imaging modalities. If that proves to be the case then routine functional precision imaging using this technique could become a clinical reality.

Acknowledgements

KMB's lab is supported by a Cancer Research UK Programme grant (17242) and by the CRUK-EPSRC Imaging Centre in Cambridge and Manchester (16465).

Table 1

Metabolite	T_1 (s)	Polarization	Measurable products	Measures	References
[1-^{13}C]pyruvate	40 (9.4 T)	>60%	[1-^{13}C]lactate, ^{13}C bicarbonate, 1-^{13}C]alanine	MCT expression, LDH, PDH and ALT activity, NADH availability	[11,77]
[1,4-$^{13}C_2$]fumarate	24 (9.4 T)	26 – 35%	[1,4-$^{13}C_2$]malate	Necrosis – leakage of fumarase from necrotic cells increases conversion of [1,4-$^{13}C_2$]fumarate to [1,4-$^{13}C_2$]malate	[60]
[1-^{13}C]lactate	45 (3 T)	7%	[1-^{13}C]pyruvate, [1-^{13}C]alanine, ^{13}C-bicarbonate	MCT expression, LDH, PDH and ALT activity, NAD^+ availability	[86]
[1-^{13}C]alanine	66 (3 T)	25	[1-^{13}C]pyruvate, [1-^{13}C]lactate	NADH availability, LDH and ALT expression	[68]
[1-^{13}C]α-ketoglutarate	52 (3 T)	16.3 ± 3%	[1-^{13}C]2-hydroxyglutarate	Mutant IDH expression, NADPH availability	[35]
[1-^{13}C]glutamine	31 (1 T)	34.7 ±7%	[1-^{13}C]2-hydroxyglutarate	Mutant IDH expression	[36]
[5-^{13}C]glutamine	16 (9.4 T)	5%	[5-^{13}C]glutamate	Glutaminase activity, glutamine transport	[29]

			^{13}C]dihydroxyacetone phosphate, ^{13}C-bicarbonate		
γ-glutamyl-[1-^{13}C]glycine	30 (9.4 T)	5.4%	[1-^{13}C]glycine	GGT activity	[38]
[1-^{13}C]acetate	16.2 (9.4 T)	13%	[1-^{13}C]acetylCoA, [1-^{13}C]acetylcarnitine	MCT expression, acetylCoA synthetase and carnitine acetyltransferase activity	[88]

Table 1. The properties of some hyperpolarized subtrates that have been used in cancer studies. The T_1 is the spin lattice relaxation time and is a measure of the polarization lifetime. The numbers in parentheses are the field strengths at which these relaxation times were measured. Abbreviations: MCT, monocarboxylate transporter; LDH, lactate dehydrogenase; PDH, pyruvate dehydrogenase; ALT, alanine transaminase; IDH, isocitrate dehydrogenase; GGT, γ-glutamyltransferase.

Figure legends

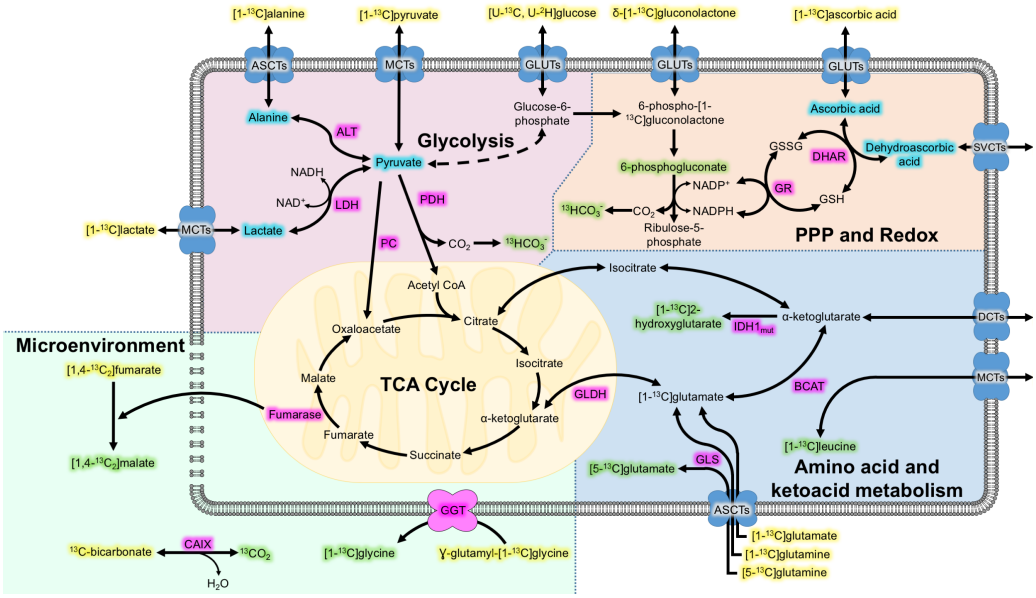

Figure 1. Metabolic processes targeted with hyperpolarized ^{13}C-labe metabolites. Color coding: pink – enzymes; yellow – hyperpolarized ^{13}C- substrates; green – measurable hyperpolarized ^{13}C-labeled products; cya hyperpolarized ^{13}C-labeled substrates and measurable products (depend substrate injected). Abbreviations: **ALT** – alanine transaminase; **ASCTs** - serine, cysteine transporters (there are also several other transporters tha transport glutamine into cells); **BCAT** – branched chain amino acid amin **CAIX** – carbonic anhydrase 9; **DCTs** – dicarboxylate transporters; **DHAR** dihydroascorbate reductase; **GGT** - ɣ-glutamyltransferase; **GLDH** – gluta dehydrogenase; **GLS** – glutaminase; **GLUTs** – glucose transporters; **GR** glutathione reductase; **GSH** – glutathione; **GSSR** – glutathione disulfide; isocitrate dehydrogenase; **LDH** – lactate dehydrogenase; **MCTs** – monoc transporters; **PC** – pyruvate carboxylase; **PDH** – pyruvate dehydrogenas pentose phosphate pathway; **SVCTs** – sodium-ascorbate co-transporters

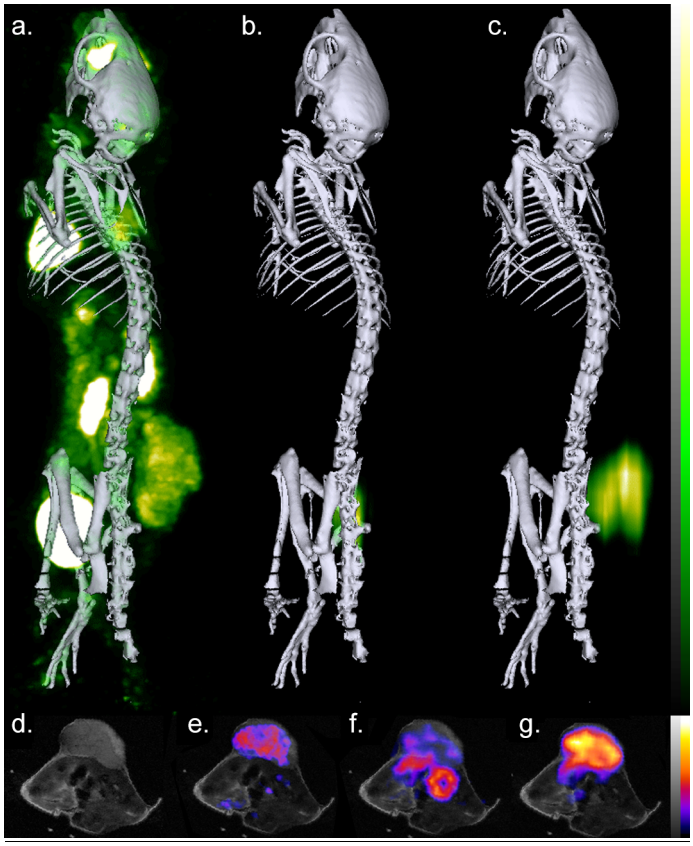

Figure 2. Combined ^{18}FDG-PET/CT and hyperpolarized [1-^{13}C]pyruvate MRI. (a-c) 3D CT bone reconstructions of a representative Colo205 tumor-bearing mouse with co-registered overlays of **(a)** ^{18}FDG, **(b)** [1-^{13}C]pyruvate and **(c)** [1-^{13}C]lactate. **(d – g)** images from a single 2.5 mm thick axial slice. **(d)** T_2-weighted fast spin echo image with overlaid with **(e)** ^{18}FDG, **(f)** [1-^{13}C]pyruvate and **(g)** [1-^{13}C]lactate images.

References

1. Warburg O PK, Negelein E.: **Über den stoffwechsel der carcinomzelle**. *Biochemische Zeitschrift* 1924, **152**:319-344.
2. Stehelin D, Varmus HE, Bishop JM, Vogt PK: **DNA related to the transforming gene(s) of avian sarcoma viruses is present in normal avian DNA**. *Nature* 1976, **260**:170-173.
•3. Hensley CT, Faubert B, Yuan Q, Lev-Cohain N, Jin E, Kim J, Jiang L, Ko B, Skelton R, Loudat L, et al.: **Metabolic Heterogeneity in Human Lung Tumors**. *Cell* 2016, **164**:681-694.
^{13}C-labeled glucose infusions in patients showed that non-small cell lung tumors have enhanced rates of both aerobic glycolysis and glucose oxidation compared to normal lung.

4. DeBerardinis RJ, Chandel NS: **Fundamentals of cancer metabolism**. *Sci Adv* 2016, **2**:e1600200.
5. Hanahan D, Weinberg RA: **Hallmarks of cancer: the next generation**. *Cell* 2011, **144**:646-674.
6. Van Dort ME, Rehemtulla A, Ross BD: **PET and SPECT Imaging of Tumor Biology: New Approaches towards Oncology Drug Discovery and Development**. *Curr Comput Aided Drug Des* 2008, **4**:46-53.
7. Lewis DY, Soloviev D, Brindle KM: **Imaging tumor metabolism using positron emission tomography**. *Cancer J* 2015, **21**:129-136.
8. Nelson SJ: **Assessment of therapeutic response and treatment planning for brain tumors using metabolic and physiological MRI**. *NMR Biomed* 2011, **24**:734-749.
¨9. Nelson SJ, Kurhanewicz J, Vigneron DB, Larson PE, Harzstark AL, Ferrone M, van Criekinge M, Chang JW, Bok R, Park I, et al.: **Metabolic imaging of patients with prostate cancer using hyperpolarized [1-(1)(3)C]pyruvate**. *Sci Transl Med* 2013, **5**:198ra108.
The first clinical hyperpolarized MRI study, using hyperpolarized [1-^{13}C]pyruvate in prostate cancer.
¨10. Aggarwal R, Vigneron DB, Kurhanewicz J: **Hyperpolarized 1-[13C]-Pyruvate Magnetic Resonance Imaging Detects an Early Metabolic Response to Androgen Ablation Therapy in Prostate Cancer**. *Eur Urol* 2017, **72**:1028-1029.
A case report showing that hyperpolarized [1-^{13}C]pyruvate can detect response to androgen ablation therapy in a patient with prostate cancer.
11. Day SE, Kettunen MI, Gallagher FA, Hu DE, Lerche M, Wolber J, Golman K, Ardenkjaer-Larsen JH, Brindle KM: **Detecting tumor response to treatment using hyperpolarized 13C magnetic resonance imaging and spectroscopy**. *Nat Med* 2007, **13**:1382-1387.
12. Brindle KM: **Imaging metabolism with hyperpolarized (13)C-labeled cell substrates**. *J Am Chem Soc* 2015, **137**:6418-6427.
˙13. Serrao EM, Kettunen MI, Rodrigues TB, Dzien P, Wright AJ, Gopinathan A, Gallagher FA, Lewis DY, Frese KK, Almeida J, et al.: **MRI with hyperpolarised [1-13C]pyruvate detects advanced pancreatic preneoplasia prior to invasive disease in a mouse model**. *Gut* 2016, **65**:465-475.
This paper demonstrated that by measuring the alanine/lactate ratio, hyperpolarized [1-^{13}C]pyruvate could be used to differentiate between the stages of development of pancreatic adenocarcinoma in a genetically engineered mouse model of the disease.
14. Keshari KR, Wilson DM: **Chemistry and biochemistry of 13C hyperpolarized magnetic resonance using dynamic nuclear polarization**. *Chem Soc Rev* 2014, **43**:1627-1659.
15. Comment A, Merritt ME: **Hyperpolarized magnetic resonance as a sensitive detector of metabolic function**. *Biochemistry* 2014, **53**:7333-7357.
16. Comment A: **Dissolution DNP for in vivo preclinical studies**. *J Magn Reson* 2016, **264**:39-48.
17. Gutte H, Hansen AE, Johannesen HH, Clemmensen AE, Ardenkjaer-Larsen JH, Nielsen CH, Kjaer A: **The use of dynamic nuclear polarization (13)C-pyruvate MRS in cancer**. *Am J Nucl Med Mol Imaging* 2015, **5**:548-560.
18. Ardenkjaer-Larsen JH, Fridlund B, Gram A, Hansson G, Hansson L, Lerche MH, Servin R, Thaning M, Golman K: **Increase in signal-to-noise ratio of >**

10,000 times in liquid-state NMR. *Proc Natl Acad Sci U S A* 2003, **100**:10158-10163.
19. Welch HG, Black WC: **Overdiagnosis in cancer**. *J Natl Cancer Inst* 2010, **102**:605-613.
20. Klotz L: **Prostate cancer overdiagnosis and overtreatment**. *Curr Opin Endocrinol Diabetes Obes* 2013, **20**:204-209.
21. Howlader N NA, Krapcho M, Miller D, Bishop K, Kosary CL, Yu M, Ruhl J, Tatalovich Z, Mariotto A, Lewis DR, Chen HS, Feuer EJ, Cronin KA: **SEER Cancer Statistics Review, 1975-2014, National Cancer Institute. Bethesda, MD,** https://seer.cancer.gov/csr/1975_2014/**, based on November 2016 SEER data submission, posted to the SEER web site, April 2017.** 2017.
¨22. Chen HY, Larson PEZ, Bok RA, von Morze C, Sriram R, Delos Santos R, Delos Santos J, Gordon JW, Bahrami N, Ferrone M, et al.: **Assessing Prostate Cancer Aggressiveness with Hyperpolarized Dual-Agent 3D Dynamic Imaging of Metabolism and Perfusion**. *Cancer Res* 2017, **77**:3207-3216.
Using the TRAMP model of prostate cancer in mice, the authors demonstrated dual agent hyperpolarization of [1-^{13}C]pyruvate and ^{13}C urea and found that high-grade tumors had higher rates of lactate production and poorer perfusion than low-grade tumors.
23. Olive KP, Tuveson DA, Ruhe ZC, Yin B, Willis NA, Bronson RT, Crowley D, Jacks T: **Mutant p53 gain of function in two mouse models of Li-Fraumeni syndrome**. *Cell* 2004, **119**:847-860.
24. Hingorani SR, Petricoin EF, Maitra A, Rajapakse V, King C, Jacobetz MA, Ross S, Conrads TP, Veenstra TD, Hitt BA, et al.: **Preinvasive and invasive ductal pancreatic cancer and its early detection in the mouse**. *Cancer Cell* 2003, **4**:437-450.
25. Hesketh RL, Zhu AX, Oklu R: **Radiomics and circulating tumor cells: personalized care in hepatocellular carcinoma?** *Diagn Interv Radiol* 2015, **21**:78-84.
26. Bode BP, Kaminski DL, Souba WW, Li AP: **Glutamine transport in isolated human hepatocytes and transformed liver cells**. *Hepatology* 1995, **21**:511-520.
27. Bode BP, Souba WW: **Modulation of cellular proliferation alters glutamine transport and metabolism in human hepatoma cells**. *Ann Surg* 1994, **220**:411-422; discussion 422-414.
28. DeBerardinis RJ, Mancuso A, Daikhin E, Nissim I, Yudkoff M, Wehrli S, Thompson CB: **Beyond aerobic glycolysis: transformed cells can engage in glutamine metabolism that exceeds the requirement for protein and nucleotide synthesis**. *Proc Natl Acad Sci U S A* 2007, **104**:19345-19350.
29. Gallagher FA, Kettunen MI, Day SE, Lerche M, Brindle KM: **13C MR spectroscopy measurements of glutaminase activity in human hepatocellular carcinoma cells using hyperpolarized 13C-labeled glutamine**. *Magn Reson Med* 2008, **60**:253-257.
30. Cabella C, Karlsson M, Canape C, Catanzaro G, Colombo Serra S, Miragoli L, Poggi L, Uggeri F, Venturi L, Jensen PR, et al.: **In vivo and in vitro liver cancer metabolism observed with hyperpolarized [5-(13)C]glutamine**. *J Magn Reson* 2013, **232**:45-52.
31. Barb AW, Hekmatyar SK, Glushka JN, Prestegard JH: **Exchange facilitated indirect detection of hyperpolarized 15ND2-amido-glutamine**. *J Magn Reson* 2011, **212**:304-310.

32. Yan H, Parsons DW, Jin G, McLendon R, Rasheed BA, Yuan W, Kos I, Batinic-Haberle I, Jones S, Riggins GJ, et al.: **IDH1 and IDH2 mutations in gliomas**. *N Engl J Med* 2009, **360**:765-773.
33. Park JM, Josan S, Jang T, Merchant M, Watkins R, Hurd RE, Recht LD, Mayer D, Spielman DM: **Volumetric spiral chemical shift imaging of hyperpolarized [2-(13) c]pyruvate in a rat c6 glioma model**. *Magn Reson Med* 2016, **75**:973-984.
•34. Izquierdo-Garcia JL, Viswanath P, Eriksson P, Cai L, Radoul M, Chaumeil MM, Blough M, Luchman HA, Weiss S, Cairncross JG, et al.: **IDH1 Mutation Induces Reprogramming of Pyruvate Metabolism**. *Cancer Res* 2015, **75**:2999-3009.
The authors used hyperpolarized [2-^{13}C]pyruvate to show that [5-^{13}C]glutamate production was decreased in IDH1 mutant cells, which was attributed to decreased pyruvate dehydrogenase activity.
•35. Chaumeil MM, Larson PE, Yoshihara HA, Danforth OM, Vigneron DB, Nelson SJ, Pieper RO, Phillips JJ, Ronen SM: **Non-invasive in vivo assessment of IDH1 mutational status in glioma**. *Nat Commun* 2013, **4**:2429.
This study showed that hyperpolarized [1-^{13}C]α-ketoglutarate could be used to detect 2-hydroxyglutarate in glioma and thus reports on the tumor IDH1 mutational status.
••36. Salamanca-Cardona L, Shah H, Poot AJ, Correa FM, Di Gialleonardo V, Lui H, Miloushev VZ, Granlund KL, Tee SS, Cross JR, et al.: **In Vivo Imaging of Glutamine Metabolism to the Oncometabolite 2-Hydroxyglutarate in IDH1/2 Mutant Tumors**. *Cell Metab* 2017.
The authors showed that glutamine was the predominant carbon source for 2-hydroxyglutarate in IDH mutant tumors and then went on to demonstrate that hyperpolarized [1-^{13}C]glutamine could be used to measure 2-hydroxyglutarate production.
37. Corti A, Franzini M, Paolicchi A, Pompella A: **Gamma-glutamyltransferase of cancer cells at the crossroads of tumor progression, drug resistance and drug targeting**. *Anticancer Res* 2010, **30**:1169-1181.
••38. Nishihara T, Yoshihara HA, Nonaka H, Takakusagi Y, Hyodo F, Ichikawa K, Can E, Bastiaansen JA, Takado Y, Comment A, et al.: **Direct Monitoring of gamma-Glutamyl Transpeptidase Activity In Vivo Using a Hyperpolarized (13) C-Labeled Molecular Probe**. *Angew Chem Int Ed Engl* 2016, **55**:10626-10629.
Here hyperpolarized ɣ-Glu-[1-^{13}C]Gly was used to measure ɣGT activity in several different normal rat organs. ɣGT is over-expressed in a several tumors and therefore this tracer has potential for use in oncology.
39. Barrington SF, Mikhaeel NG, Kostakoglu L, Meignan M, Hutchings M, Mueller SP, Schwartz LH, Zucca E, Fisher RI, Trotman J, et al.: **Role of imaging in the staging and response assessment of lymphoma: consensus of the International Conference on Malignant Lymphomas Imaging Working Group**. *J Clin Oncol* 2014, **32**:3048-3058.
40. Gallamini A, Zwarthoed C: **Interim FDG-PET Imaging in Lymphoma**. *Semin Nucl Med* 2018, **48**:17-27.
41. Cheson BD, Fisher RI, Barrington SF, Cavalli F, Schwartz LH, Zucca E, Lister TA, Alliance AL, Lymphoma G, Eastern Cooperative Oncology G, et al.: **Recommendations for initial evaluation, staging, and response**

assessment of Hodgkin and non-Hodgkin lymphoma: the Lugano classification. *J Clin Oncol* 2014, **32**:3059-3068.
42. Sachpekidis C, Larribere L, Pan L, Haberkorn U, Dimitrakopoulou-Strauss A, Hassel JC: **Predictive value of early 18F-FDG PET/CT studies for treatment response evaluation to ipilimumab in metastatic melanoma: preliminary results of an ongoing study**. *Eur J Nucl Med Mol Imaging* 2015, **42**:386-396.
43. McArthur GA, Puzanov I, Amaravadi R, Ribas A, Chapman P, Kim KB, Sosman JA, Lee RJ, Nolop K, Flaherty KT, et al.: **Marked, homogeneous, and early [18F]fluorodeoxyglucose-positron emission tomography responses to vemurafenib in BRAF-mutant advanced melanoma**. *J Clin Oncol* 2012, **30**:1628-1634.
44. Seith F, Forschner A, Schmidt H, Pfannenberg C, Guckel B, Nikolaou K, la Fougere C, Garbe C, Schwenzer N: **18F-FDG-PET detects complete response to PD1-therapy in melanoma patients two weeks after therapy start**. *Eur J Nucl Med Mol Imaging* 2018, **45**:95-101.
45. Cho SY, Lipson EJ, Im HJ, Rowe SP, Gonzalez EM, Blackford A, Chirindel A, Pardoll DM, Topalian SL, Wahl RL: **Prediction of Response to Immune Checkpoint Inhibitor Therapy Using Early-Time-Point (18)F-FDG PET/CT Imaging in Patients with Advanced Melanoma**. *J Nucl Med* 2017, **58**:1421-1428.
46. Siegel JA, Pennington CW, Sacks B: **Subjecting Radiologic Imaging to the Linear No-Threshold Hypothesis: A Non Sequitur of Non-Trivial Proportion**. *J Nucl Med* 2017, **58**:1-6.
47. Aliaga A, Rousseau JA, Cadorette J, Croteau E, van Lier JE, Lecomte R, Benard F: **A small animal positron emission tomography study of the effect of chemotherapy and hormonal therapy on the uptake of 2-deoxy-2-[F-18]fluoro-D-glucose in murine models of breast cancer**. *Mol Imaging Biol* 2007, **9**:144-150.
48. Balasubramanian Harisankar CN, Preethi R, John J: **Metabolic flare phenomenon on 18 fluoride-fluorodeoxy glucose positron emission tomography-computed tomography scans in a patient with bilateral breast cancer treated with second-line chemotherapy and bevacizumab**. *Indian J Nucl Med* 2015, **30**:145-147.
49. Mortimer JE, Dehdashti F, Siegel BA, Trinkaus K, Katzenellenbogen JA, Welch MJ: **Metabolic flare: indicator of hormone responsiveness in advanced breast cancer**. *J Clin Oncol* 2001, **19**:2797-2803.
50. Witney TH, Kettunen MI, Day SE, Hu DE, Neves AA, Gallagher FA, Fulton SM, Brindle KM: **A comparison between radiolabeled fluorodeoxyglucose uptake and hyperpolarized (13)C-labeled pyruvate utilization as methods for detecting tumor response to treatment**. *Neoplasia* 2009, **11**:574-582, 571 p following 582.
51. Witney TH, Kettunen MI, Hu DE, Gallagher FA, Bohndiek SE, Napolitano R, Brindle KM: **Detecting treatment response in a model of human breast adenocarcinoma using hyperpolarised [1-13C]pyruvate and [1,4-13C2]fumarate**. *Br J Cancer* 2010, **103**:1400-1406.
52. Harris T, Eliyahu G, Frydman L, Degani H: **Kinetics of hyperpolarized 13C1-pyruvate transport and metabolism in living human breast cancer cells**. *Proc Natl Acad Sci U S A* 2009, **106**:18131-18136.

53. Saito K, Matsumoto S, Takakusagi Y, Matsuo M, Morris HD, Lizak MJ, Munasinghe JP, Devasahayam N, Subramanian S, Mitchell JB, et al.: **13C-MR Spectroscopic Imaging with Hyperpolarized [1-13C]pyruvate Detects Early Response to Radiotherapy in SCC Tumors and HT-29 Tumors**. *Clin Cancer Res* 2015, **21**:5073-5081.
54. Delgado-Goni T, Miniotis MF, Wantuch S, Parkes HG, Marais R, Workman P, Leach MO, Beloueche-Babari M: **The BRAF Inhibitor Vemurafenib Activates Mitochondrial Metabolism and Inhibits Hyperpolarized Pyruvate-Lactate Exchange in BRAF-Mutant Human Melanoma Cells**. *Mol Cancer Ther* 2016, **15**:2987-2999.
55. Hu S, Balakrishnan A, Bok RA, Anderton B, Larson PE, Nelson SJ, Kurhanewicz J, Vigneron DB, Goga A: **13C-pyruvate imaging reveals alterations in glycolysis that precede c-Myc-induced tumor formation and regression**. *Cell Metab* 2011, **14**:131-142.
56. Park I, Mukherjee J, Ito M, Chaumeil MM, Jalbert LE, Gaensler K, Ronen SM, Nelson SJ, Pieper RO: **Changes in pyruvate metabolism detected by magnetic resonance imaging are linked to DNA damage and serve as a sensor of temozolomide response in glioblastoma cells**. *Cancer Res* 2014, **74**:7115-7124.
57. Ravoori MK, Singh SP, Lee J, Bankson JA, Kundra V: **In Vivo Assessment of Ovarian Tumor Response to Tyrosine Kinase Inhibitor Pazopanib by Using Hyperpolarized 13C-Pyruvate MR Spectroscopy and 18F-FDG PET/CT Imaging in a Mouse Model**. *Radiology* 2017, **285**:830-838.
58. Neveu MA, De Preter G, Joudiou N, Bol A, Brender JR, Saito K, Kishimoto S, Gregoire V, Jordan BF, Krishna MC, et al.: **Multi-modality imaging to assess metabolic response to dichloroacetate treatment in tumor models**. *Oncotarget* 2016, **7**:81741-81749.
•59. Duwel S, Durst M, Gringeri CV, Kosanke Y, Gross C, Janich MA, Haase A, Glaser SJ, Schwaiger M, Schulte RF, et al.: **Multiparametric human hepatocellular carcinoma characterization and therapy response evaluation by hyperpolarized (13) C MRSI**. *NMR Biomed* 2016, **29**:952-960.
In an orthotopic model of hepatocellular carcinoma the authors demonstrated the use of [1-^{13}C]pyruvate, [1, 4-$^{13}C_2$]fumarate and [^{13}C,$^{15}N_2$]urea to detect response to trans-arterial embolization.
60. Gallagher FA, Kettunen MI, Hu DE, Jensen PR, Zandt RI, Karlsson M, Gisselsson A, Nelson SK, Witney TH, Bohndiek SE, et al.: **Production of hyperpolarized [1,4-13C2]malate from [1,4-13C2]fumarate is a marker of cell necrosis and treatment response in tumors**. *Proc Natl Acad Sci U S A* 2009, **106**:19801-19806.
61. Kato Y, Ozawa S, Miyamoto C, Maehata Y, Suzuki A, Maeda T, Baba Y: **Acidic extracellular microenvironment and cancer**. *Cancer Cell Int* 2013, **13**:89.
62. Gallagher FA, Sladen H, Kettunen MI, Serrao EM, Rodrigues TB, Wright A, Gill AB, McGuire S, Booth TC, Boren J, et al.: **Carbonic Anhydrase Activity Monitored In Vivo by Hyperpolarized 13C-Magnetic Resonance Spectroscopy Demonstrates Its Importance for pH Regulation in Tumors**. *Cancer Res* 2015, **75**:4109-4118.
63. Gallagher FA, Kettunen MI, Day SE, Hu DE, Ardenkjaer-Larsen JH, Zandt R, Jensen PR, Karlsson M, Golman K, Lerche MH, et al.: **Magnetic resonance imaging of pH in vivo using hyperpolarized 13C-labelled bicarbonate**. *Nature* 2008, **453**:940-943.

64. Shchepin RV, Barskiy DA, Coffey AM, Theis T, Shi F, Warren WS, Goodson BM, Chekmenev EY: **(15)N Hyperpolarization of Imidazole-(15)N2 for Magnetic Resonance pH Sensing via SABRE-SHEATH**. *ACS Sens* 2016, **1**:640-644.
65. Jiang W, Lumata L, Chen W, Zhang S, Kovacs Z, Sherry AD, Khemtong C: **Hyperpolarized 15N-pyridine derivatives as pH-sensitive MRI agents**. *Sci Rep* 2015, **5**:9104.
¨66. Duwel S, Hundshammer C, Gersch M, Feuerecker B, Steiger K, Buck A, Walch A, Haase A, Glaser SJ, Schwaiger M, et al.: **Imaging of pH in vivo using hyperpolarized 13C-labelled zymonic acid**. *Nat Commun* 2017, **8**:15126.
The pH dependent chemical shift of [1, 5-$^{13}C_2$]zymonic acid was demonstrated to be an accurate *in vivo* extracellular pH probe in normal rat organs.
67. Rodic S, Vincent MD: **Reactive oxygen species (ROS) are a key determinant of cancer's metabolic phenotype**. *Int J Cancer* 2018, **142**:440-448.
68. Park JM, Khemtong C, Liu SC, Hurd RE, Spielman DM: **In vivo assessment of intracellular redox state in rat liver using hyperpolarized [1-13 C]Alanine**. *Magn Reson Med* 2017, **77**:1741-1748.
69. Timm KN, Hartl J, Keller MA, Hu DE, Kettunen MI, Rodrigues TB, Ralser M, Brindle KM: **Hyperpolarized [U-(2) H, U-(13) C]Glucose reports on glycolytic and pentose phosphate pathway activity in EL4 tumors and glycolytic activity in yeast cells**. *Magn Reson Med* 2015, **74**:1543-1547.
70. Rodrigues TB, Serrao EM, Kennedy BW, Hu DE, Kettunen MI, Brindle KM: **Magnetic resonance imaging of tumor glycolysis using hyperpolarized 13C-labeled glucose**. *Nat Med* 2014, **20**:93-97.
71. Moreno KX, Harrison CE, Merritt ME, Kovacs Z, Malloy CR, Dean Sherry A: **Hyperpolarized delta-[1-13 C]gluconolactone as a probe of the pentose phosphate pathway**. *NMR Biomed* 2017, **30**.
72. Keshari KR, Kurhanewicz J, Bok R, Larson PE, Vigneron DB, Wilson DM: **Hyperpolarized 13C dehydroascorbate as an endogenous redox sensor for in vivo metabolic imaging**. *Proc Natl Acad Sci U S A* 2011, **108**:18606-18611.
73. Bohndiek SE, Kettunen MI, Hu DE, Kennedy BW, Boren J, Gallagher FA, Brindle KM: **Hyperpolarized [1-13C]-ascorbic and dehydroascorbic acid: vitamin C as a probe for imaging redox status in vivo**. *J Am Chem Soc* 2011, **133**:11795-11801.
˙74. Timm KN, Hu DE, Williams M, Wright AJ, Kettunen MI, Kennedy BW, Larkin TJ, Dzien P, Marco-Rius I, Bohndiek SE, et al.: **Assessing Oxidative Stress in Tumors by Measuring the Rate of Hyperpolarized [1-13C]Dehydroascorbic Acid Reduction Using 13C Magnetic Resonance Spectroscopy**. *J Biol Chem* 2017, **292**:1737-1748.
This study showed that hyperpolarized [1-^{13}C]dehydroascorbic acid could be used to assess oxidative stress in tumors, and the rate of DHA reduction was dependent on the rate of NADPH production.
75. Wang J, Wright AJ, Hu DE, Hesketh R, Brindle KM: **Single shot three-dimensional pulse sequence for hyperpolarized 13 C MRI**. *Magn Reson Med* 2017, **77**:740-752.
76. Milshteyn E, von Morze C, Reed GD, Shang H, Shin PJ, Zhu Z, Chen HY, Bok R, Goga A, Kurhanewicz J, et al.: **Development of high resolution 3D hyperpolarized carbon-13 MR molecular imaging techniques**. *Magn Reson Imaging* 2017, **38**:152-162.

77. Yoshihara HA, Can E, Karlsson M, Lerche MH, Schwitter J, Comment A: **High-field dissolution dynamic nuclear polarization of [1-(13)C]pyruvic acid**. *Phys Chem Chem Phys* 2016, **18**:12409-12413.
•78. Ji X, Bornet A, Vuichoud B, Milani J, Gajan D, Rossini AJ, Emsley L, Bodenhausen G, Jannin S: **Transportable hyperpolarized metabolites**. *Nat Commun* 2017, **8**:13975.
One of the practical challenges in translation of hyperpolarized MRI is the siting of the hyperpolarizer. Here the authors demonstrate that separation of the hyperpolarized substrate from the radical significantly prolongs the half-lives, permitting transport or storage of the hyperpolarized material.
•79. Capozzi A, Cheng T, Boero G, Roussel C, Comment A: **Thermal annihilation of photo-induced radicals following dynamic nuclear polarization to produce transportable frozen hyperpolarized 13C-substrates**. *Nat Commun* 2017, **8**:15757.
Here the authors use a photo-induced radical to polarize [1-^{13}C]pyruvate and then use thermal annihilation to remove the radical, producing a pure substrate with signinficantly prolonged hyperpolarization.
80. Wang J, Kreis F, Wright AJ, Hesketh RL, Levitt MH, Brindle KM: **Dynamic 1 H imaging of hyperpolarized [1-13 C]lactate in vivo using a reverse INEPT experiment**. *Magn Reson Med* 2017.
81. Ehman EC, Johnson GB, Villanueva-Meyer JE, Cha S, Leynes AP, Larson PEZ, Hope TA: **PET/MRI: Where might it replace PET/CT?** *J Magn Reson Imaging* 2017, **46**:1247-1262.
82. Gutte H, Hansen AE, Larsen MM, Rahbek S, Johannesen HH, Ardenkjaer-Larsen J, Kristensen AT, Hojgaard L, Kjaer A: **In Vivo Phenotyping of Tumor Metabolism in a Canine Cancer Patient with Simultaneous (18)F-FDG-PET and Hyperpolarized (13)C-Pyruvate Magnetic Resonance Spectroscopic Imaging (hyperPET): Mismatch Demonstrates that FDG may not Always Reflect the Warburg Effect**. *Diagnostics (Basel)* 2015, **5**:287-289.
•83. Gutte H, Hansen AE, Larsen MM, Rahbek S, Henriksen ST, Johannesen HH, Ardenkjaer-Larsen J, Kristensen AT, Hojgaard L, Kjaer A: **Simultaneous Hyperpolarized 13C-Pyruvate MRI and 18F-FDG PET (HyperPET) in 10 Dogs with Cancer**. *J Nucl Med* 2015, **56**:1786-1792.
In this canine study, the feasibility of simultaneous ^{18}FDG-PET and hyperpolarized [1-^{13}C]pyruvate studies was demonstrated, with most tumors demonstrating a correlation between [1-^{13}C]lactate production and ^{18}FDG uptake.
84. Eldirdiri A, Clemmensen A, Bowen S, Kjaer A, Ardenkjaer-Larsen JH: **Simultaneous imaging of hyperpolarized [1,4-13 C2]fumarate, [1-13 C]pyruvate and 18 F-FDG in a rat model of necrosis in a clinical PET/MR scanner**. *NMR Biomed* 2017, **30**.
85. Gutte H, Hansen AE, Henriksen ST, Johannesen HH, Ardenkjaer-Larsen J, Vignaud A, Hansen AE, Borresen B, Klausen TL, Wittekind AM, et al.: **Simultaneous hyperpolarized (13)C-pyruvate MRI and (18)F-FDG-PET in cancer (hyperPET): feasibility of a new imaging concept using a clinical PET/MRI scanner**. *Am J Nucl Med Mol Imaging* 2015, **5**:38-45.
86. Chen AP, Kurhanewicz J, Bok R, Xu D, Joun D, Zhang V, Nelson SJ, Hurd RE, Vigneron DB: **Feasibility of using hyperpolarized [1-13C]lactate as a substrate for in vivo metabolic 13C MRSI studies**. *Magn Reson Imaging* 2008, **26**:721-726.

87. Gallagher FA, Kettunen MI, Day SE, Hu DE, Karlsson M, Gisselsson A, Lerche MH, Brindle KM: **Detection of tumor glutamate metabolism in vivo using (13)C magnetic resonance spectroscopy and hyperpolarized [1-(13)C]glutamate**. *Magn Reson Med* 2011, **66**:18-23.
88. Bastiaansen JA, Cheng T, Mishkovsky M, Duarte JM, Comment A, Gruetter R: **In vivo enzymatic activity of acetylCoA synthetase in skeletal muscle revealed by (13)C turnover from hyperpolarized [1-(13)C]acetate to [1-(13)C]acetylcarnitine**. *Biochim Biophys Acta* 2013, **1830**:4171-4178.